Efficiency Potential of Photovoltaic Materials and Devices Unveiled by Detailed-Balance Analysis

Uwe Rau,[1,*] Beatrix Blank,[1] Thomas C. M. Müller,[1] and Thomas Kirchartz[1,2]

[1]*IEK5-Photovoltaik, Forschungszentrum Jülich, 52425 Jülich, Germany*

[2]*Faculty of Engineering and CENIDE, University of Duisburg-Essen, Carl-Benz-Strasse 199, 47057 Duisburg, Germany*

(Received 16 November 2016; revised manuscript received 8 February 2017; published 19 April 2017)

A consistent mathematical approach is presented that connects the Shockley-Queisser (SQ) theory to the analysis of real-world devices. We demonstrate that the external photovoltaic quantum efficiency Q_e^{PV} of a solar cell results from a distribution of SQ-type band-gap energies and how this distribution is derived from experimental data. This leads us to the definition of a photovoltaic band-gap energy E_g^{PV} as a reference value for the analysis of the device performance. For a variety of solar-cell devices, we show that the combination of Q_e^{PV} and electroluminescence measurements allows for a detailed loss analysis that is fully compatible with the principle of detailed balance.

DOI: 10.1103/PhysRevApplied.7.044016

I. INTRODUCTION

The Shockley-Queisser (SQ) theory [1] provides a definite description of the upper efficiency limit of photovoltaic energy conversion by a single semiconductor material with thermalized charge carriers. The rigorous application of the principle of detailed balance [2] shown therein has subsequently inspired other researchers to develop ideas on how to go beyond [3–6] the implications given by the SQ theory as well as to strive for generalizations towards real-world devices [7–10]. The latter point has become especially important, as recent years have seen amazing progress in various photovoltaic technologies like world records for $\mathrm{Cu(In,Ga)Se_2}$ [11,12], crystalline c-Si [13,14], and GaAs [13,15] solar cells, and the rise of metal-halide perovskites materials [16–18]. The SQ limit gives us a reference value for comparison with the achievements of specific photovoltaic devices [19–26].

The convenience of the model assumption behind the SQ theory, in the following denoted specifically as the SQ *model*, lies in the fact that they require only one physical quantity as the input parameter, the band-gap energy E_g of the photovoltaic absorber material. However, the price for this simplification is a very specific definition of E_g (in the following denoted as the Shockley-Queisser gap E_g^{SQ}). This definition results from describing the dependence of the absorptance A of the photovoltaic absorber material on the photon energy E as a step function. The ingenuity of this approach condones its physical impossibility: Such an absorptance is not achievable by any real semiconductor device. The difference between the idealized situation and real materials or devices may be small in some cases but can also be very large, as we show below. An important ingredient of the SQ approach is to look at the solar cell from the outside; i.e., the solar cell is described by area-related quantities exclusively. The connection between the physical volume properties of real photovoltaic absorber materials and the limiting efficiency was done for the case of silicon by Tiedje *et al.* in 1984 [8]. In 1997, Marti *et al.* [27] finally conciliated the SQ model with Shockley's diode equation by considering photon recycling as the decisive mechanism connecting radiative recombination in the bulk of the semiconductor given by the van Roosbroek–Shockley equation [28] with the emission through the cell's surface. Thus, the SQ model is consistently connected to the framework of bulk semiconductor physics. However, the mathematics needed to relate the inside of the semiconductor with the outside world is somewhat involved (see, e.g., Ref. [29]), and cursory approaches recently led to false conclusions [30] that required corrections [31]. In contrast, the optoelectronic reciprocity theorem [32] greatly facilitates the theoretical and experimental analysis of solar cells because it relates (like the SQ model) only externally measurable quantities with each other and bypasses the complicated inside-outside connections.

The present paper proposes a mathematically consistent and physically meaningful extension of the SQ theory connecting it to the physics of real-world devices without the need to consider the complex connection between bulk- and surface-related properties. This extension interprets any measured absorptance $A(E)$ of photovoltaic materials and any measured external photovoltaic quantum efficiency $Q_e^{\mathrm{PV}}(E)$ of photovoltaic devices as a result of a distribution $P(E_g^{\mathrm{SQ}})$ of SQ-type band-gap energies. We show how this distribution is directly determined from experimental data.

*Corresponding author.
u.rau@fz-juelich.de

Combining the method with measured luminescence data finally allows one to quantify the photovoltaic potential of materials and devices in terms of radiative and nonradiative losses.

II. GENERALIZED SHOCKLEY-QUEISSER MODEL

A. Optoelectronic reciprocity

In order to apply the general idea of the SQ theorem to real devices with non-step-function-like absorptances or quantum efficiencies, a generalization of the concept is needed. This is provided by the optoelectronic reciprocity theorem [32] connecting the electroluminescent emission $\phi_{\mathrm{em}}(E)$ of a solar cell with its photovoltaic quantum efficiency via

$$\phi_{\mathrm{em}}(E) = Q_e^{\mathrm{PV}}(E)\phi_{\mathrm{BB}}(E)\left\{\exp\left(\frac{qV}{kT}\right) - 1\right\}. \quad (1)$$

Here, $\phi_{\mathrm{BB}}(E)$ denotes the blackbody spectrum at temperature T of the cell, k is Boltzmann's constant, and q the elementary charge. Integrating the electroluminescent emission over energy and multiplication with q yields the radiative emission current density that follows a diode law with the radiative saturation current density given by

$$J_0^{\mathrm{rad}} = q\int_{-\infty}^{\infty} Q_e^{\mathrm{PV}}(E)\phi_{\mathrm{BB}}(E)dE. \quad (2)$$

The short-circuit current density J_{SC} of a solar cell is written in an analogous form

$$J_{\mathrm{SC}} = q\int_{-\infty}^{\infty} Q_e^{\mathrm{PV}}(E)\phi_{\mathrm{Sun}}(E)dE, \quad (3)$$

where $\phi_{\mathrm{Sun}}(E)$ denotes the solar spectrum. Note that Eqs. (2) and (3) assume that Q_e^{PV} is independent from the incident angle, otherwise, angular dependence must be included. Note further that the integrals formally cover an energy range from $-\infty$ to ∞ allowing for the use of the derivation theorem for convolutions (needed below), while unphysical negative energies are avoided by keeping all functions within the integral equal to zero for $E \leq 0$.

Equations (2) and (3) generalize the SQ model to all situations where the solar cell can be described in the framework of detailed balance (i.e., a linear extrapolation of thermal equilibrium to a nonequilibrium situation). Finally, setting $Q_e^{\mathrm{PV}}(E) = A(E) = H(E - E_g^{\mathrm{SQ}})$ with the Heaviside function $H(E - E_g^{\mathrm{SQ}}) = 1$ for $E > E_g^{\mathrm{SQ}}$ and $H(E - E_g^{\mathrm{SQ}}) = 0$, otherwise, Eqs. (2) and (3) yield the SQ model.

B. Distribution of band-gap energies

Another pathway [10] to generalize the original SQ theory is the assumption of a distribution $P(E_g^{\mathrm{SQ}})$ of SQ-type band-gap energies. The original idea of Ref. [10] was to investigate the influence of variations of band-gap energies, e.g., in a semiconductor alloy, on the radiative efficiency limit. Specifically, a Gaussian distribution $P_G(E_g^{\mathrm{SQ}}, \sigma_{Eg})$ was assumed, and the standard deviation σ_{Eg} was taken as a measure for the fluctuations. However, the approach is valid also for general distributions $P(E_g^{\mathrm{SQ}})$. Instead of Eqs. (2) and (3), we may write for the saturation and short-circuit current densities

$$\begin{aligned} J_{0/\mathrm{SC}}^{\mathrm{rad}/-} &= q\int_{-\infty}^{\infty} P(E_g)\int_{Eg}^{\infty} \phi_{\mathrm{BB/Sun}}(E)dEdE_g \\ &= q\int_{-\infty}^{\infty} \phi_{\mathrm{BB/Sun}}(E)\int_{-\infty}^{\infty} P(E_g)H(E - E_g)dE_g dE. \end{aligned} \quad (4)$$

Comparing the second line of Eq. (4) with Eqs. (2) and (3) allows us to write

$$Q_e^{\mathrm{PV}}(E) = \int_{-\infty}^{\infty} P(E_g)H(E - E_g)dE_g. \quad (5)$$

Thus, Eq. (5) suggests interpreting the external quantum efficiency $Q_e^{\mathrm{PV}}(E)$ as the result of a distribution of SQ-type band-gap energies. Finally, taking the derivative of Eq. (5) with respect to photon energy E leads to

$$\begin{aligned} \frac{d}{dE}Q_e^{\mathrm{PV}}(E) &= \int_{-\infty}^{\infty} P(E_g)\frac{d}{dE}H(E - E_g)dE_g \\ &= \int_{-\infty}^{\infty} P(E_g)\delta(E - E_g)dE_g = P(E). \end{aligned} \quad (6)$$

In Eq. (6), we use the derivation theorem for convolutions and the fact that the derivative of the Heaviside function $H(E - E_g)$ is the δ function $\delta(E - E_g)$. Thus, the derivative of the external quantum efficiency $Q_e^{\mathrm{PV}}(E)$ with respect to the photon energy equals the band-gap distribution of band-gap energies, i.e., $P(E_g) = P(E)$. Thus, with Eq. (6), $P(E_g)$ can easily be determined from any experimentally obtained quantum efficiency spectrum $Q_e^{\mathrm{PV}}(E)$ by taking its derivative as illustrated in Fig. 1.

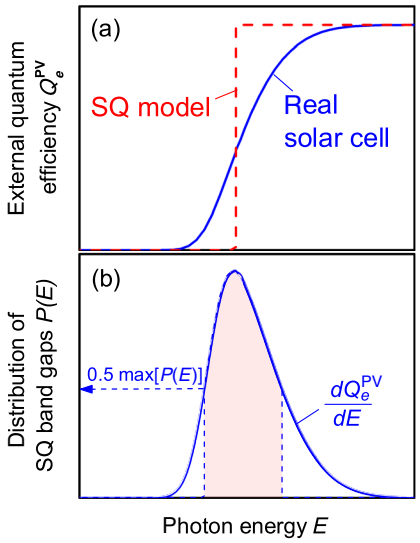

FIG. 1. The proposed analysis of practical devices uses the measured external quantum efficiency $Q_e^{\mathrm{PV}}(E)$ [blue curve in (a)] and interprets its derivative [blue curve in (b)] as a distribution of SQ-type band gaps. From the distribution $P(E)$, the photovoltaic gap E_g^{PV} is determined. The steplike quantum efficiency [red curve in (a)] then defines the reference values J_0^{SQ} and $J_{\mathrm{SC}}^{\mathrm{SQ}}$ for SQ-type open-circuit voltage $V_{\mathrm{OC}}^{\mathrm{SQ}}$.

C. Photovoltaic band-gap definition

In the next step, we define the photovoltaic band-gap energy E_g^{PV} as the mean peak energy at the absorption edge of the distribution $P(E_g)$,

$$E_g^{\mathrm{PV}} = \int_a^b E_g P(E_g) dE_g \Big/ \int_a^b P(E_g) dE_g, \tag{7}$$

where the integration limits a and b are chosen as the energy where $P(E_g)$ is equal to 50% of its maximum, $P(a) = P(b) = \max[P(E_g)]/2$ as exemplarily depicted in Fig. 3(e). This restriction of the integration limits is not motivated physically but rather by practical reasons as it avoids the influence of noisy data at low energies as well as negative values for $P(E_g)$ in the case of $dQ_e^{\mathrm{PV}}(E)/dE < 0$ at high energies. Thus, our definition of the integration limits should be understood as a convention for the determination of the band-gap energy E_g^{PV} applicable to any solar cell. Furthermore, E_g^{PV} represents an *external* property of a photovoltaic device and not an (internal) property of a photovoltaic material as, e.g., the Tauc gap [33]. We note that a definition of the band gap similar to our proposition was given earlier by Aiken *et al.* [34]. Helmers *et al.* [35] criticized this definition as "unphysical" and introduced their own procedure for the analysis of the temperature dependence of band-gap energies in multijunction solar cells. This approach might serve better the purpose of analyzing the temperature dependence of the direct band gaps because it aims at internal semiconductor properties. However, the external definition via a distribution of SQ-type band-gap energies as proposed here aims at a consistent analysis of losses for a solar cell entirely from its external properties. Figure 2 compares the band gaps determined using the maximum of the SQ band-gap distribution $P(E)$ (red diamonds), Eq. (7) (blue half-filled circles), the Helmers *et al.* method (green squares), and the Tauc method (yellow triangle). For a short description of the latter two methods, see Appendix A.

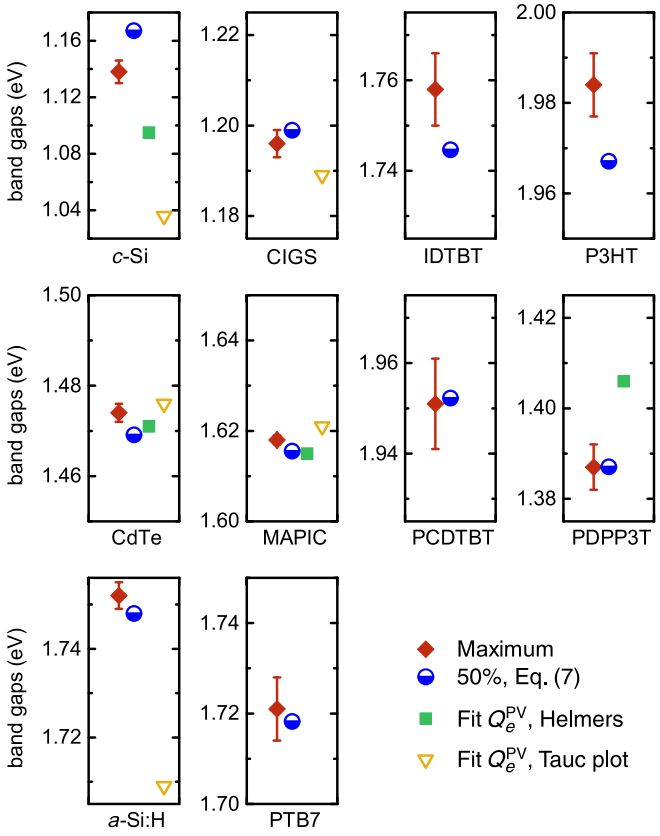

FIG. 2. Photovoltaic band gaps of ten organic and inorganic, direct and indirect semiconductors as defined by Eq. (7) (blue half-filled circles), the maximum of the derivative of the Q_e^{PV} (red diamonds), a fit to the Q_e^{PV} as introduced by Helmers *et al.* [35] (green squares), and the Tauc plot [33] (yellow triangle).

Thus, with E_g^{PV} we gain an effective energy defining SQ-type reference values for the saturation current densities $J_0^{\mathrm{SQ}}(E_g^{\mathrm{PV}})$ and $J_{\mathrm{SC}}^{\mathrm{SQ}}(E_g^{\mathrm{PV}})$. Both quantities are determined in the classical way via substituting $Q_e^{\mathrm{PV}}(E)$ by the unit step function $H(E - E_g^{\mathrm{SQ}})$ in Eqs. (2) and (3). Finally, we determine the open-circuit voltage

$$V_{\mathrm{OC}}^{\mathrm{SQ}}(E_g^{\mathrm{PV}}) = \frac{kT_c}{q} \ln\left(\frac{J_{\mathrm{SC}}^{\mathrm{SQ}}(E_g^{\mathrm{PV}})}{J_0^{\mathrm{SQ}}(E_g^{\mathrm{PV}})}\right) \tag{8}$$

as a reference value.

D. Quantifying loss mechanisms

Following Ross [36] and later works [32,37] the open-circuit voltage of a solar cell can be separated into a radiative open-circuit voltage V_{OC}^{rad} and a nonradiative loss term via

$$V_{OC} = \frac{kT_c}{q}\ln\left(\frac{J_{SC}}{J_0}\right) = \frac{kT_c}{q}\ln\left(\frac{J_{SC}}{J_0^{rad}}\times\frac{J_0^{rad}}{J_0}\right) = V_{OC}^{rad} + \frac{kT_c}{q}\ln\left(\frac{J_0^{rad}}{J_0}\right) = V_{OC}^{rad} + \frac{kT_c}{q}\ln(Q_{LED}^{e}), \tag{9}$$

where Q_{LED}^{e} denotes the external luminescence or light-emitting-diode quantum efficiency. The combination of Eq. (9) with Eqs. (1)–(3) [23,24,38] allows one to compare nonradiative losses in solar cells across all technologies based on a common theoretical framework and has been used in various publications [22–26,38–45]. Note that for this type of voltage-loss analysis, it is common to assume that the photocurrent $J_{ph}(V=0) = J_{SC}$ is voltage independent (see the Supplemental Material of Ref. [22]).

With the definitions from Sec. II C, we expand the expression Eq. (9) for the open-circuit voltage V_{OC} for any given photovoltaic device in a well-defined way by

$$V_{OC} = \frac{kT_c}{q}\ln\left(\frac{J_{SC}}{J_0}\right) = \frac{kT_c}{q}\ln\left(\frac{J_{SC}^{SQ}}{J_0^{SQ}}\times\frac{J_{SC}}{J_{SC}^{SQ}}\times\frac{J_0^{SQ}}{J_0^{rad}}\times\frac{J_0^{rad}}{J_0}\right). \tag{10}$$

The three last quotients within the ln argument can be associated with a loss term ΔV_{OC}^{x} according to

$$V_{OC} = V_{OC}^{SQ} - \Delta V_{OC}^{SC} - \Delta V_{OC}^{rad} - \Delta V_{OC}^{nonrad}. \tag{11}$$

In Eq. (11), we have with $V_{OC}^{SQ}(E_g^{PV})$, as defined in Eq. (8), a reference quantity uniquely defined by the photovoltaic band-gap energy E_g^{PV}. Since the open-circuit voltage can be understood as the asymptotic energy turnover per incident photon (i.e., each excess electron-hole pair photogenerated and collected under open-circuit conditions delivers an energy qV_{OC} at the terminals of the device) [46], each loss term ΔV_{OC}^{x} in Eq. (11) corresponds to an entropy-generation term $\sigma_x = q\Delta V_{OC}^{x}/T$.

The short-circuit loss term $\Delta V_{OC}^{SC} = kT_c/q \times \ln(J_{SC}^{SQ}/J_{SC})$ results from the difference between the real short-circuit current density J_{SC} and the theoretical value J_{SC}^{SQ} that is defined by a step-function-like external quantum efficiency. As this difference for most solar cells amounts to some 10% at most, the resulting open-circuit voltage loss is small (though the loss in overall performance might be significant). In contrast, the radiative loss term $\Delta V_{OC}^{rad} = kT_c/q \times \ln(J_0^{rad}/J_0^{SQ})$ can amount to hundreds of millivolts [22]. This is because an energy shift of the luminescent emission with respect to the photovoltaic band-gap energy E_g^{PV} leads to a J_0^{rad} that can be orders of magnitude larger than J_0^{SQ}; see, also, Fig. S1 in the Supplemental Material [47]. Finally, the nonradiative loss term $\Delta V_{OC}^{nonrad} = kT_c/q \times \ln(J_0/J_0^{rad})$ corresponds to the difference between the actual V_{OC} of the device and the open-circuit voltage $V_{OC}^{rad} = kT_C/q \times \ln(J_{SC}/J_0^{rad})$ in the radiative limit. The difference ΔV_{OC}^{nonrad} is related to the external electroluminescence quantum efficiency Q_e^{LED} of the device via [32,36,37] $\Delta V_{OC}^{nonrad} = -kT_c/q \times \ln(Q_e^{LED})$, a relation that has been proven in the past to be extraordinarily useful for the direct, quantitative comparison of different solar-cell technologies [22–26,40–43,45] and for the analysis of light-trapping schemes in photovoltaic devices [31,48,49].

III. APPLICATION TO VARIOUS PHOTOVOLTAIC TECHNOLOGIES

Figure 3 shows external quantum efficiencies Q_e^{PV} in black, the normalized distribution of SQ band gaps obtained from dQ_e^{PV}/dE in blue, and the measured electroluminescence (EL) spectra ϕ_{EL} in red for solar cells with different absorber materials [crystalline (c-Si), $Cu(In,Ga)Se_2$ (CIGS), CdTe, $CH_3NH_3PbI_{3-x}Cl_x$ (MAPIC), hydrogenated amorphous silicon (a-Si:H),

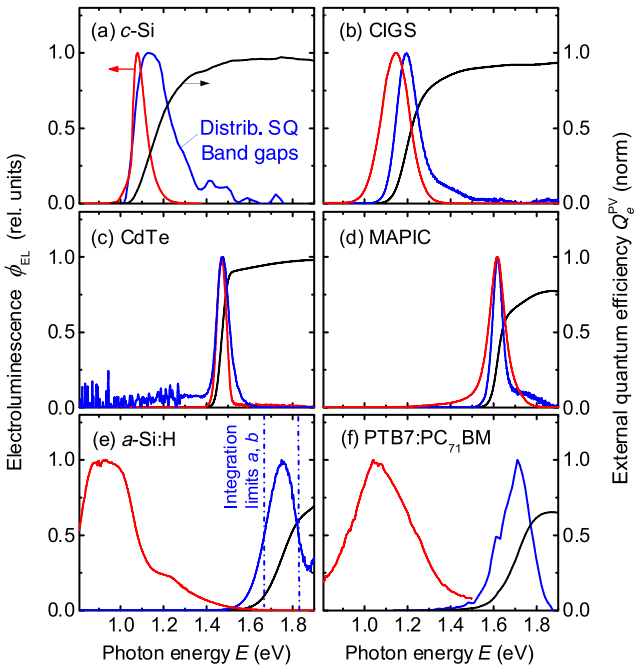

FIG. 3. External quantum efficiency Q_e (black) and the respective distribution of SQ band gaps (blue) and EL emission (red) of six different technologies. The distribution of the SQ band gaps as well as the EL emission is broader for c-Si and CIGS than for CdTe and MAPIC. The broadest distributions are found for a-Si:H and PTB7:PC_{71}BM with a significant peak shift between SQ band-gap distribution and EL emission.

and the organic polymer-fullerene blend poly [(4,8-bis-(2-ethylhexyloxy)-benzo(1,2−b:4,5-b′)dithiophene)-2,6-diyl-alt-(4-(2-ethylhexyl)-3-fluorothieno[3,4-b]thiophene-)-2-carboxylate-2-6-diyl)] (PTB7):[6, 6]-phenyl C_{71} butyric acid methyl ester ($PC_{71}BM$)]. The Q_e^{PV} is either determined via Fourier-transform photocurrent spectroscopy measurements [Figs. 3(b)–3(e)] or taken from Ref. [38] in the case of *c*-Si and Ref. [22] in the case of PTB7:$PC_{71}BM$. The *c*-Si and the CIGS samples display a broader distribution $P(E_g)$ of band gaps compared to those of CdTe and MAPIC which display the sharpest SQ-gap distribution and the sharpest EL emission spectra. The widening of the CIGS distribution results from band-gap grading of the direct band gap [24], whereas the widening of the *c*-Si distribution results from the indirect nature of the *c*-Si band gap and the consequent phononic distributions to the radiative transitions [25] as well as the influence of light trapping in the long-wavelength range [48]. The photovoltaic gap energy E_g^{PV} for the *c*-Si cell (1.17 eV) obtained from $P(E_g^{SQ})$ is slightly larger than the band-gap energy E_g (1.12 eV) defined by the density of states of an ideal silicon crystal. This difference results from the fact that the definition of E_g^{PV} is functional with respect to the photovoltaic action of the device. Such functional definitions of band-gap energies are especially used for disordered materials where different analysis methods lead to different gaps for different functional purposes.

Unsurprisingly, for the case of the *a*-Si:H device, $E_g^{PV} = 1.75$ eV is closer to the optical band gap than to the mobility gap (typically, 1.7 eV determined via the activation energy of the conductivity of intrinsic material) [50]. The *a*-Si:H as well as the PTB7:$PC_{71}BM$ cells show the broadest EL spectra and SQ-gap distributions as well as the largest difference between the two. In *a*-Si:H, this energy shift between absorption and emission is due to the prevailing emission by radiative band-to-dangling bond recombination [51–54]. In PTB7:$PC_{71}BM$, the shift between absorption and emission is attributed to radiative emission involving the charge-transfer state between the two organic components which is energetically lower than the dominant absorption contribution of the pure polymer or fullerene [22,55].

In organic solar cells, the difference between the absorption onset as determined by a fit to the absorption edge or quantum efficiency and the actually measured V_{OC} is often used as a figure of merit [39,56–60]. Substantial efforts are currently directed towards achieving high photocurrents for low differences between absorption onset and V_{OC} [39,43–45,58,59]. A disadvantage of the approach used in the literature is the requirement to extract the optical band gap from a fit that is typically done to UV-vis data. This procedure is not well defined and leaves room for personal interpretation but directly affects the obtained value for $E_g - qV_{OC}$ that is used to assess a certain material combination. Using the concept of a photovoltaic band gap as proposed here does not require additional measurements (quantum efficiencies are typically reported in the community) and allows a reproducible definition of the energy loss $E_g - qV_{OC}$.

To obtain V_{OC}^{SQ} for all cells, we determine the photovoltaic gap E_g^{SQ} with Eq. (7) and the quantities J_{SC}^{SQ} and J_0^{SQ} according to Eqs. (2) and (3) [for a single band-gap distribution $P(E_g) = \delta(E - E_g^{PV})$] with the help of tabulated values for the solar spectrum AM1.5g [61] and from Planck's equation for temperature $T = 300$ K. Analogously, we calculate J_{SC} and J_0^{rad} with the help of Eq. (1) from the measured quantum efficiencies. We note that for the latter step the validity of Eq. (1) is required and should be checked experimentally by comparing the measured Q_e^{PV} values with those calculated from the EL emission [24,38,47,62]. However, some solar cells do not fulfill Eq. (1) [54,63,64]. This is the case for the *a*-Si:H cell in the present work where radiative recombination rates change nonlinearly with increasing voltage bias [54]. However, the concept of a radiative ideality factor n_{rad} [54,65] provides the possibility to calculate V_{OC}^{SQ} in spite of this complication, as shown in Appendix B.

Figure 4 summarizes the open-circuit voltage losses ΔV_{OC}^{rad}, ΔV_{OC}^{SC}, and ΔV_{OC}^{nonrad} for different solar cells. The largest radiative losses ΔV_{OC}^{rad} are present in P3HT:$PC_{61}BM$ as expected for the observed large shift between absorption and emission (see the Supplemental Material [66] for P3HT:$PC_{61}BM$). For *c*-Si and CIGS, these losses are moderate for reasons discussed above. The virtual absence ΔV_{OC}^{rad} in Fig. 4 because of its extremely sharp optical absorption edge is considered a primary quality of MAPIC as a photovoltaic material [22,67]. For comparison, the voltage losses of GaAs are shown with data taken from Table I in Ref. [22]. Note that the optical band gap in this

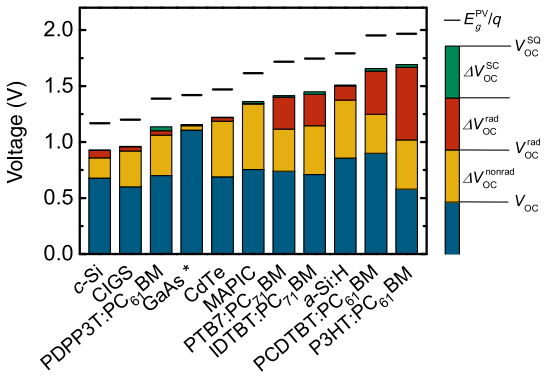

FIG. 4. Open-circuit voltage losses ΔV_{OC}^{SC} due to a nonideal short-circuit current density (green), ΔV_{OC}^{rad} due to radiative recombination (red), and ΔV_{OC}^{nonrad} due to nonradiative recombination for a variety of different solar-cell technologies. The SQ band gap is indicated by a black line and the measured V_{OC} as a blue bar. *Voltage loss data of GaAs are taken from Ref. [22].

case is not determined via Eq. (7); however, the band-gap edge of GaAs is that sharp that the application of any reasonable definition of the band-gap energy results in the same value within the error. GaAs exhibits the smallest overall losses in voltage of only $V_{\mathrm{OC}}^{\mathrm{SQ}} - V_{\mathrm{OC}} \approx 47$ mV. The short-circuit loss term $\Delta V_{\mathrm{OC}}^{\mathrm{SC}}$ is small for all devices, though one should keep in mind that carrier collection losses showing up in J_{SC} become painful when considering the device efficiency. Finally, the nonradiative losses $\Delta V_{\mathrm{OC}}^{\mathrm{nonrad}}$ strongly depend on the optimization of the materials and the devices. Except for the *c*-Si sample, these losses are relatively large in all devices presented here but are substantially reduced when considering champion devices [23].

IV. SUMMARY

In summary, the concept of a distribution of SQ gaps bridges the gap between the idealization underlying the SQ theory and the physical properties of any real-world photovoltaic device. The concept is the basis for a quantitative and intuitive detailed-balance analysis of thermodynamic losses that can be readily applied to any solar cell. The extension of this concept for the analysis of photovoltaic absorber materials without the need to prepare a device or for the analysis of material properties obtained by computational materials research is straightforward.

ACKNOWLEDGMENTS

The authors acknowledge support from the DFG (Grants No. KI-1571/2-1 and No. RA 473/7-1) and from the Helmholtz Association via the Helmholtz-NREL Solar Energy Initiative. B. B. thanks the Bosch-Forschungsstiftung for a Ph.D. scholarship.

APPENDIX A: DIFFERENT DEFINITIONS OF BAND GAP FROM THE Q_e^{PV}

We compare our definition of the photovoltaic band gap given by Eq. (7) with two other methods published earlier in the literature, namely, a slight modification of the well-known Tauc plot [33] and a method introduced by Helmers *et al.* [35] in Fig. 2. In the following, we give a brief summary of these methods; please see the referenced literature for a more detailed description.

Tauc [33]: We use the approximation $Q_e^{\mathrm{PV}} \sim A \sim \alpha$ for small αd where A denotes the absorptance, α the absorption coefficient, and d the thickness of the absorber layer. We then plot the quantity $(\alpha E)^k$ over the photon energy E. For indirect semiconductors, the exponent is $k = 1/2$, whereas for direct semiconductors $k = 2$. The band-gap energies are determined by extrapolation of the linear region of this plot to the abscissa. The band-gap energies derived by this method are shown for all inorganic semiconductors in Fig. 2 (yellow triangles).

Helmers *et al.* [35]: On a logarithmic plot of the Q_e^{PV}, a linear function is fitted to the low-energy edge of the Q_e^{PV} as well as to the saturation plateau for higher energies. The intercept of the two functions determines the band-gap energy. For all devices where this method seems applicable to us, because the data show this linear behavior on a logarithmic scale (see Ref. [47] Fig. S1 and Ref. [66] Fig. S2), the values determined by Helmers's method are also shown in Fig. 2 (green squares).

APPENDIX B: RADIATIVE IDEALITY FACTORS >1

If band-to-band recombination is not the dominant radiative recombination path in the device, luminescence does not scale with $\exp(qV/kT)$, and the relation $V_{\mathrm{OC}}^{\mathrm{rad}} - V_{\mathrm{OC}} = -kT_c/q \times \ln(Q_e^{\mathrm{LED}})$ is not valid anymore. Therefore, we need a generalization of $V_{\mathrm{OC}}^{\mathrm{rad}}$ for solar-cell technologies with nonideal luminescence via band-to-dangling bond or tail-to-tail recombination, e.g., *a*-Si:H [68]. In the case of nonideal luminescent emission, we may still describe the dependence of the EL intensity Φ_{EL} on internal voltage with $\Phi_{\mathrm{EL}} \propto \exp(qV/n_{\mathrm{rad}}kT)$. The radiative limit $V_{\mathrm{OC}}^{\mathrm{rad}}$ can then be consistently described using the radiative ideality factor n_{rad} [65,68],

$$V_{\mathrm{OC}}^{\mathrm{rad}} = \frac{n_{\mathrm{rad}} kT_c}{q} \ln\left(\frac{J_{\mathrm{SC}}}{J_0^{\mathrm{rad}}}\right). \tag{B1}$$

Note that the nonideality of radiative recombination has no effect on the idealized voltage limits by Shockley-Queisser [1]. The difference between the SQ case and the nonideal radiative limit then reads

$$\begin{aligned} V_{\mathrm{OC}}^{\mathrm{SQ}} - V_{\mathrm{OC}}^{\mathrm{rad}} &= \frac{kT_c}{q}\left[\ln\left(\frac{J_{\mathrm{SC}}^{\mathrm{SQ}}}{J_{\mathrm{SC}}}\right) + \ln\left(\frac{J_0^{\mathrm{rad}}}{J_0^{\mathrm{SQ}}}\right) \right. \\ &\quad \left. - \left(n_{\mathrm{rad}} - 1\right)\ln\left(\frac{J_{\mathrm{SC}}}{J_0^{\mathrm{rad}}}\right)\right] \\ &= \Delta V_{\mathrm{OC}}^{\mathrm{SC}} + \Delta V_{\mathrm{OC}}^{\mathrm{rad,id}} - \Delta V_{\mathrm{OC}}^{\mathrm{rad,corr}}. \end{aligned} \tag{B2}$$

Thus, the radiative loss term $\Delta V_{\mathrm{OC}}^{\mathrm{rad}} = \Delta V_{\mathrm{OC}}^{\mathrm{rad,id}} - \Delta V_{\mathrm{OC}}^{\mathrm{rad,corr}}$ is obtained from the ideal value $\Delta V_{\mathrm{OC}}^{\mathrm{rad,id}}$ by correcting $\Delta V_{\mathrm{OC}}^{\mathrm{rad,corr}}$ for the nonideality of radiative recombination. To calculate the nonradiative voltage loss $\Delta V_{\mathrm{OC}}^{\mathrm{nonrad}} = V_{\mathrm{OC}}^{\mathrm{rad}} - V_{\mathrm{OC}}$, we have to take the ideality factor $n_{\mathrm{id}} > 1$ into account, because the open-circuit voltage is given by $V_{\mathrm{OC}} = (n_{\mathrm{id}} kT_c/q)\ln(J_{\mathrm{SC}}/J_0)$. Consequently, we obtain

$$\begin{aligned} \Delta V_{\mathrm{OC}}^{\mathrm{nonrad}} &= V_{\mathrm{OC}}^{\mathrm{rad}} - V_{\mathrm{OC}} \\ &= -\frac{n_{\mathrm{rad}} kT_c}{q}\left[-\ln\left(\frac{J_{\mathrm{SC}}}{J_0^{\mathrm{rad}}}\right) + \frac{n_{\mathrm{id}}}{n_{\mathrm{rad}}}\ln\left(\frac{J_{\mathrm{SC}}}{J_0}\right)\right]. \end{aligned} \tag{B3}$$

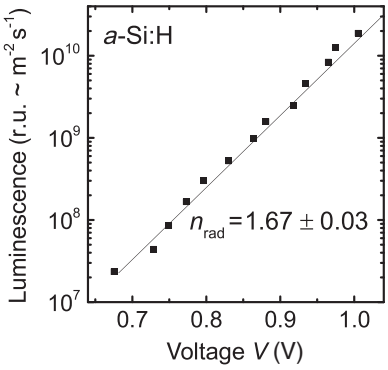

FIG. 5. Determination of the radiative ideality factor of a-Si:H by voltage-dependent electroluminescence.

Using $J_{SC} = J_0 \exp(qV_{OC}/n_{id}kT_c)$, we can simplify the term and find for the nonideal case ($n_{id} \neq 1$ and $n_{rad} \neq 1$),

$$\Delta V_{OC}^{nonrad} = -\frac{n_{rad}kT_c}{q} \ln\left(\frac{J_0^{rad} \exp(qV_{OC}/n_{rad}kT_c)}{J_0 \exp(qV_{OC}/n_{id}kT_c)}\right) = -\frac{n_{rad}kT_c}{q} \ln(Q_e^{LED}).$$

The radiative ideality factor for the a-Si:H cell is $n_{rad} = 1.67 \mp 0.3$; see Fig. 5. The voltage losses for a-Si:H in Fig. 4 are accordingly calculated using Eq. (B1).

[1] W. Shockley and H. J. Queisser, Detailed balance limit of efficiency of p-n junction solar cells, J. Appl. Phys. **32**, 510 (1961).

[2] P. W. Bridgman, Note on the principle of detailed balancing, Phys. Rev. **31**, 101 (1928).

[3] J. H. Werner, S. Kolodinski, and H. J. Queisser, Novel Optimization Principles and Efficiency Limits for Semiconductor Solar Cells, Phys. Rev. Lett. **72**, 3851 (1994).

[4] M. A. Green, Third generation photovoltaics: Ultra-high conversion efficiency at low cost, Prog. Photovoltaics **9**, 123 (2001).

[5] M. A. Green, Third generation photovoltaics: Solar cells for 2020 and beyond, Physica (Amsterdam) **14E**, 65 (2002).

[6] A. Luque and A. Marti, Increasing the Efficiency of Ideal Solar Cells by Photon Induced Transitions at Intermediate Levels, Phys. Rev. Lett. **78**, 5014 (1997).

[7] M. A. Green, Limits on the open-circuit voltage and efficiency of silicon solar cells imposed by intrinsic Auger processes, IEEE Trans. Electron Devices **31**, 671 (1984).

[8] T. Tiedje, E. Yablonovitch, G. D. Cody, and B. G. Brooks, Limiting efficiency of silicon solar cells, IEEE Trans. Electron Devices **31**, 711 (1984).

[9] T. Kirchartz, K. Taretto, and U. Rau, Efficiency limits of organic bulk heterojunction solar cells, J. Phys. Chem. C **113**, 17958 (2009).

[10] U. Rau and J. H. Werner, Radiative efficiency limits of solar cells with lateral band-gap fluctuations, Appl. Phys. Lett. **84**, 3735 (2004).

[11] P. Jackson, D. Hariskos, R. Wuerz, O. Kiowski, A. Bauer, T. M. Friedlmeier, and M. Powalla, Properties of $Cu(In, Ga)Se_2$ solar cells with new record efficiencies up to 21.7%, Phys. Status Solidi RRL **9**, 28 (2015).

[12] P. Jackson, R. Wuerz, D. Hariskos, E. Lotter, W. Witte, and M. Powalla, Effects of heavy alkali elements in $Cu(In, Ga)Se_2$ solar cells with efficiencies up to 22.6%, Phys. Status Solidi RRL **10**, 583 (2016).

[13] M. A. Green, K. Emery, Y. Hishikawa, W. Warta, and E. D. Dunlop, Solar cell efficiency tables (Version 45), Prog. Photovoltaics **23**, 1 (2015).

[14] K. Yoshikawa, H. Kawasaki, W. Yoshida, T. Irie, K. Konishi, K. Nakano, T. Uto, D. Adachi, M. Kanematsu, H. Uzu, and K. Yamamoto, Nat. Energy **2**, 17032 (2017).

[15] B. M. Kayes, H. Nie, R. Twist, S. G. Spruytte, F. Reinhardt, I. C. Kizilyalli, and G. S. Higashi, in Proceedings of the *37th IEEE Photovoltaic Specialists Conference* (IEEE, Piscataway, 2011), p. 000004.

[16] N. J. Jeon, J. H. Noh, W. S. Yang, Y. C. Kim, S. Ryu, J. Seo, and S. I. Seok, Compositional engineering of perovskite materials for high-performance solar cells, Nature (London) **517**, 476 (2015).

[17] W. S. Yang, J. H. Noh, N. J. Jeon, Y. C. Kim, S. Ryu, J. Seo, and S. I. Seok, High-performance photovoltaic perovskite layers fabricated through intramolecular exchange, Science **348**, 1234 (2015).

[18] M. Saliba, T. Matsui, K. Domanski, J. Y. Seo, A. Ummadisingu, S. M. Zakeeruddin, J. P. Correa-Baena, W. R. Tress, A. Abate, A. Hagfeldt *et al.*, Incorporation of rubidium cations into perovskite solar cells improves photovoltaic performance, Science **354**, 206 (2016).

[19] L. C. Hirst and N. J. Ekins-Daukes, Fundamental losses in solar cells, Prog. Photovoltaics **19**, 286 (2011).

[20] P. K. Nayak, J. Bisquert, and D. Cahen, Assessing possibilities and limits for solar cells, Adv. Mater. **23**, 2870 (2011).

[21] P. K. Nayak, G. Garcia-Belmonte, A. Kahn, J. Bisquert, and D. Cahen, Photovoltaic efficiency limits and material disorder, Energy Environ. Sci. **5**, 6022 (2012).

[22] J. Z. Yao, T. Kirchartz, M. S. Vezie, M. A. Faist, W. Gong, Z. C. He, H. B. Wu, J. Troughton, T. Watson, D. Bryant *et al.*, Quantifying Losses in Open-Circuit Voltage in Solution-Processable Solar Cells, Phys. Rev. Applied **4**, 014020 (2015).

[23] M. A. Green, Radiative efficiency of state-of-the-art photovoltaic cells, Prog. Photovoltaics **20**, 472 (2012).

[24] T. Kirchartz and U. Rau, Electroluminescence analysis of high efficiency $Cu(In, Ga)Se_2$ solar cells, J. Appl. Phys. **102**, 104510 (2007).

[25] T. Kirchartz, A. Helbig, W. Reetz, M. Reuter, J. H. Werner, and U. Rau, Reciprocity between electroluminescence and quantum efficiency used for the characterization of silicon solar cells, Prog. Photovoltaics **17**, 394 (2009).

[26] W. Tress, N. Marinova, O. Inganas, M. K. Nazeeruddin, S. M. Zakeeruddin, and M. Graetzel, Predicting the open-circuit voltage of $CH_3NH_3PbI_3$ perovskite solar cells using electroluminescence and photovoltaic quantum efficiency

spectra: The role of radiative and non-radiative recombination, Adv. Energy Mater. **5**, 1400812 (2015).
[27] A. Marti, J. L. Balenzategui, and R. F. Reyna, Photon recycling and Shockley's diode equation, J. Appl. Phys. **82**, 4067 (1997).
[28] W. van Roosbroeck and W. Shockley, Photon-radiative recombination of electrons and holes in germanium, Phys. Rev. **94**, 1558 (1954).
[29] J. Mattheis, J. H. Werner, and U. Rau, Finite mobility effects on the radiative efficiency limit of *p-n* junction solar cells, Phys. Rev. B **77**, 085203 (2008).
[30] A. Polman and H. A. Atwater, Photonic design principles for ultrahigh-efficiency photovoltaics, Nat. Mater. **11**, 174 (2012).
[31] U. Rau and T. Kirchartz, On the thermodynamics of light trapping in solar cells, Nat. Mater. **13**, 103 (2014).
[32] U. Rau, Reciprocity relation between photovoltaic quantum efficiency and electroluminescent emission of solar cells, Phys. Rev. B **76**, 085303 (2007).
[33] J. Tauc, Optical properties and electronic structure of amorphous Ge and Si, Mater. Res. Bull. **3**, 37 (1968).
[34] D. Aiken, M. Stan, C. Murray, P. Sharps, J. Hills, and B. Clevenger, in *Proceedings of the Twenty-Ninth IEEE Photovoltaic Specialists Conference* (IEEE, Piscataway, New Jersey, 2002), p. 828.
[35] H. Helmers, C. Karcher, and A. W. Bett, Bandgap determination based on electrical quantum efficiency, Appl. Phys. Lett. **103**, 032108 (2013).
[36] R. T. Ross, Some thermodynamics of photochemical systems, J. Chem. Phys. **46**, 4590 (1967).
[37] G. Smestad and H. Ries, Luminescence and current voltage characteristics of solar cells and optoelectronic Devices, Sol. Energy Mater. Sol. Cells **25**, 51 (1992).
[38] T. Kirchartz, U. Rau, M. Kurth, J. Mattheis, and J. H. Werner, Comparative study of electroluminescence from $Cu(In, Ga)Se_2$ and Si solar cells, Thin Solid Films **515**, 6238 (2007).
[39] Y. X. Li, X. D. Liu, F. P. Wu, Y. Zhou, Z. Q. Jiang, B. Song, Y. X. Xia, Z. G. Zhang, F. Gao, O. Inganas *et al.*, Non-fullerene acceptor with low energy loss and high external quantum efficiency: Towards high performance polymer solar cells, J. Mater. Chem. A **4**, 5890 (2016).
[40] K. Vandewal, K. Tvingstedt, A. Gadisa, O. Inganas, and J. V. Manca, On the origin of the open-circuit voltage of polymer-fullerene solar cells, Nat. Mater. **8**, 904 (2009).
[41] K. Tvingstedt, O. Malinkiewicz, A. Baumann, C. Deibel, H. J. Snaith, V. Dyakonov, and H. J. Bolink, Radiative efficiency of lead iodide based perovskite solar cells, Sci. Rep. **4**, 6071 (2014).
[42] D. Bi, W. Tress, M. I. Dar, P. Gao, J. Luo, C. m. Renevier, K. Schenk, A. Abate, F. Giordano, J. P. Correa Baena *et al.*, Efficient luminescent solar cells based on tailored mixed-cation perovskites, Sci. Adv. **2**, e1501170 (2016).
[43] D. Baran, M. S. Vezie, N. Gasparini, F. Deledalle, J. Yao, B. C. Schroeder, H. Bronstein, T. Ameri, T. Kirchartz, I. McCulloch *et al.*, Role of polymer fractionation in energetic losses and charge carrier lifetimes of polymer: Fullerene solar cells, J. Phys. Chem. C **119**, 19668 (2015).
[44] D. Baran, T. Kirchartz, S. Wheeler, S. Dimitrov, M. Abdelsamie, J. Gorman, R. S. Ashraf, S. Holliday, A. Wadsworth, N. Gasparini *et al.*, Reduced voltage losses yield 10% efficient fullerene free organic solar cells with >1 V open circuit voltages, Energy Environ. Sci. **9**, 3783 (2016).
[45] W. Zhao, D. Qian, S. Zhang, S. Li, O. Inganas, F. Gao, and J. Hou, Fullerene-free polymer solar cells with over 11% efficiency and excellent thermal stability, Adv. Mater. **28**, 4734 (2016).
[46] T. Markvart, Thermodynamics of losses in photovoltaic conversion, Appl. Phys. Lett. **91**, 064102 (2007).
[47] See Supplemental Material at http://link.aps.org/supplemental/10.1103/PhysRevApplied.7.044016 for a discussion on the validity of the reciprocity theorem for the devices shown in Fig. S1.
[48] U. Rau, U. W. Paetzold, and T. Kirchartz, Thermodynamics of light management in photovoltaic devices, Phys. Rev. B **90**, 035211 (2014).
[49] O. D. Miller, E. Yablonovitch, and S. R. Kurtz, Strong internal and external luminescence as solar cells approach the Shockley-Queisser limit, IEEE J. Photovoltaics **2**, 303 (2012).
[50] A. V. Shah, H. Schade, M. Vanecek, J. Meier, E. Vallat-Sauvain, N. Wyrsch, U. Kroll, C. Droz, and J. Bailat, Thin-film silicon solar cell technology, Prog. Photovoltaics **12**, 113 (2004).
[51] R. A. Street, Recombination in *a*-Si:H: Defect luminescence, Phys. Rev. B **21**, 5775 (1980).
[52] R. A. Street, Luminescence and recombination in hydrogenated amorphous silicon, Adv. Phys. **30**, 593 (1981).
[53] R. A. Street, D. K. Biegelsen, and R. L. Weisfield, Recombination in *a*-Si:H: Transitions through defect states, Phys. Rev. B **30**, 5861 (1984).
[54] T. C. M. Müller, B. E. Pieters, T. Kirchartz, R. Carius, and U. Rau, Effect of localized states on the reciprocity between quantum efficiency and electroluminescence in $Cu(In, Ga)Se_2$ and Si thin-film solar cells, Sol. Energy Mater. Sol. Cells **129**, 95 (2014).
[55] K. Tvingstedt, K. Vandewal, A. Gadisa, F. L. Zhang, J. Manca, and O. Inganas, Electroluminescence from charge transfer states in polymer solar cells, J. Am. Chem. Soc. **131**, 11819 (2009).
[56] W. W. Li, K. H. Hendriks, A. Furlan, M. M. Wienk, and R. A. J. Janssen, High quantum efficiencies in polymer solar cells at energy losses below 0.6 eV, J. Am. Chem. Soc. **137**, 2231 (2015).
[57] K. Kawashima, Y. Tamai, H. Ohkita, I. Osaka, and K. Takimiya, High-efficiency polymer solar cells with small photon energy loss, Nat. Commun. **6**, 10085 (2015).
[58] N. A. Ran, J. A. Love, C. J. Takacs, A. Sadhanala, J. K. Beavers, S. D. Collins, Y. Huang, M. Wang, R. H. Friend, G. C. Bazan *et al.*, Harvesting the full potential of photons with organic solar cells, Adv. Mater. **28**, 1482 (2016).
[59] S. M. Tuladhar, M. Azzouzi, F. Delval, J. Yao, A. A. Y. Guilbert, T. Kirchartz, N. F. Montcada, R. Dominguez, F. Langa, E. Palomares *et al.*, Low open-circuit voltage loss in solution-processed small-molecule organic solar cells, ACS Energy Lett. **1**, 302 (2016).
[60] J. Liu, S. Chen, D. Qian, B. Gautam, G. Yang, J. Zhao, J. Bergqvist, F. Zhang, W. Ma, H. Ade *et al.*, Fast charge

separation in a non-fullerene organic solar cell with a small driving force, Nat. Energy **1**, 16089 (2016).

[61] American Society for Testing and Materials (ASTM) Terrestrial Reference Spectra for PV Performance Evaluation, http://rredc.nrel.gov/solar/spectra/am1.5/.

[62] U. Rau, Superposition and reciprocity in the electroluminescence and photoluminescence of solar cells, IEEE J. Photovoltaics **2**, 169 (2012).

[63] W. Gong, M. A. Faist, N. J. Ekins-Daukes, Z. Xu, D. D. C. Bradley, J. Nelson, and T. Kirchartz, Influence of energetic disorder on electroluminescence emission in polymer: fullerene solar cells, Phys. Rev. B **86**, 024201 (2012).

[64] T. Kirchartz, J. Nelson, and U. Rau, Reciprocity between Charge Injection and Extraction and Its Influence on the Interpretation of Electroluminescence Spectra in Organic Solar Cells, Phys. Rev. Applied **5**, 054003 (2016).

[65] T. M. H. Tran, B. E. Pieters, M. Schneemann, T. C. M. Müller, A. Gerber, T. Kirchartz, and U. Rau, Quantitative evaluation method for electroluminescence images of *a*-Si:H thin-film solar modules, Phys. Status Solidi RRL **7**, 627 (2013).

[66] See Supplemental Material at http://link.aps.org/supplemental/10.1103/PhysRevApplied.7.044016, Fig. S2 for the spectra of P3HT:PCBM and a few other organic materials and the key to the abbreviations of the used molecules.

[67] S. De Wolf, J. Holovsky, S. J. Moon, P. Löper, B. Niesen, M. Ledinsky, F. J. Haug, J. H. Yum, and C. Ballif, Organometallic halide perovskites: Sharp optical absorption edge and its relation to photovoltaic performance, J. Phys. Chem. Lett. **5**, 1035 (2014).

[68] T. C. M. Müller, B. E. Pieters, T. Kirchartz, R. Carius, and U. Rau, Effect of localized states on the reciprocity between quantum efficiency and electroluminescence in $Cu(In,Ga)Se_2$ and Si thin-film solar cells, Sol. Energy Mater. Sol. Cells **129**, 95 (2014).